MSc in Photonics

PHOTONICS**BCN**

Universitat Politècnica de Catalunya (UPC)
Universitat Autònoma de Barcelona (UAB)
Universitat de Barcelona (UB)
Institut de Ciències Fotòniques (ICFO)

http://www.photonicsbcn.eu

Master in Photonics

MASTER THESIS WORK

Characterization of a rapid scan FTIR for ultrafast probing in the mid-IR region

David Moreno Mencía

Supervised by Prof. Dr. Simon Wall (ICFO)

Presented on date 9th September 2016

Registered at

Escola Tècnica Superior d'Enginyeria de Telecomunicació de Barcelona

Characterization of a rapid scan FTIR for ultrafast probing in the mid-IR region

David Moreno Mencía

ICFO-The Institute of Photonic Sciences, Av. Carl Friedrich Gauss, 3, 08860, Castelldefels, Barcelona - SPAIN

E-mail: momed1292@gmail.com

September 2016

Abstract. The properties of materials in the mid-infrared spectral region (3-15μm) is vital for understanding their operation and performance. It is challenging to characterize femtosecond pulses in this spectral region. In this project, we build a simple Fourier Transform Infrared spectrometer to measure ultrafast infrared laser pulses. Due to the measurements in the mid-infared region is difficult, we demonstrate the functionality of the spectrometer at the visible region, where it has been characterized the autocorrelation, the pulse duration and the central wavelength of the pulse.

Keywords: FTIR, mid-infrared, ultrafast dynamics, femtosecond laser.

1. Introduction

Observing how light interacts with solids to generate charges is vital for understanding physics of solids, especially in the field of solar cell where trap states can localize electrons and prevent efficient extraction of the photoinduced charges.

Direct band-to-band absorption can take place only at frequencies for which the photon energy $h\nu > E_g$, where E_g is the energy gap. This adds to the concentration of mobile charge carriers and increases the conductivity of the material.

The radiative electron-hole recombination is unlikely in an indirect-gap semiconductor. This is because transitions from near the bottom of the conduction band to near the top of the valence band requires an exchange of momentum that cannot be accommodated by the emitted photon. Momentum may be conserved, however, by the participation of phonons in the interaction. Although photon absorption also requires energy and momentum conservation in an indirect-gap semiconductor, this is readily achieved by means of a two-step process. The electron is first excited to a high energy level within the conduction band by a vertical transition. It then quickly relaxes to the bottom of the conduction band by thermalization in which its momentum is transferred to phonons. These electrons have a long life time and can be extracted to generate electricity. However, it is important to understand how these photoexcited electrons

behave. As these processes occur on picosecond timescales, we need probes that can resolve femtosecond dynamics [1].

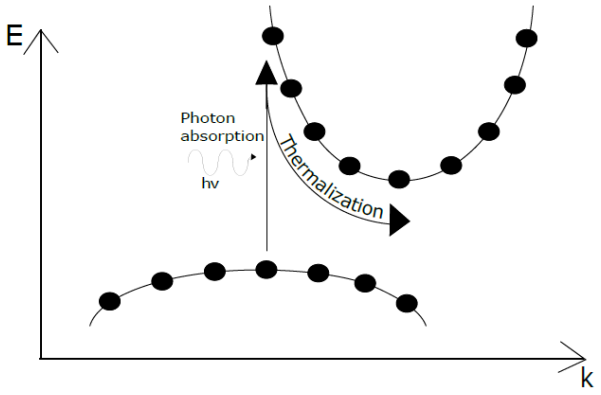

Figure 1. Photon absorption in an indirect-gap semiconductor. First, the electron is excited to a high energy level, and then it relaxes to the bottom of the conduction band by thermalization. These processes occur on picosecond timescale.

There are two extreme possibilities to explain how electrons move in the conduction band: the Drude model and polarons.

The Drude model treats electrons as free, that undergo scattering after a characteristic scattering time τ_t [2].
An striking implication of the free carrier models is that the dielectric constant $\epsilon_r(\omega) = 1 - \frac{\omega_p^2 \tau_t^2}{1+\omega^2\tau_t^2} + i\frac{\omega_p^2 \tau_t}{\omega(1+\omega^2\tau_t^2)}$ changes from being negative to positive as we go through the plasma frequency $\omega_p = \sqrt{Ne^2/\epsilon_0 m}$. This means that the reflectivity $R = \left|\frac{\sqrt{\epsilon(\omega)}-1}{\sqrt{\epsilon(\omega)}+1}\right|^2$ ceases above ω_p and some of the light can be transmitted through the solid [3][4].

Typical metals have $\omega_p = 10$ eV, but we are photoexciting so this value is much lower. The Figure 2a shows the real and imaginary part of the dielectric constant, we can see at $\omega_p = 0.7$ eV the real part of the dielectric constant changes from negative to positive and the reflectivity ceases at this frequency in figure 2b, where also a comparative plot at different number densities N is also shown [5].

On the other hand, the photoexcited electron can attract the close positive ions and repels the negative ones, it produces a local displacement of the lattice in the immediate vicinity of the electron. The lattice distortion accompanies the electron as it moves through the solid. The electron with its local lattice distortion is equivalent to a new elementary excitation of the solid, and is called a polaron [4].

To be more specific, the atoms move from their equilibrium positions to effectively screen the charge of an electron, known as a phonon cloud. This lowers the electron mobility and increases the electron's effective mass. If we want to move this electron we have to provide some energy to the system. The amount of energy supplied is in the mid-infrared (MIR).

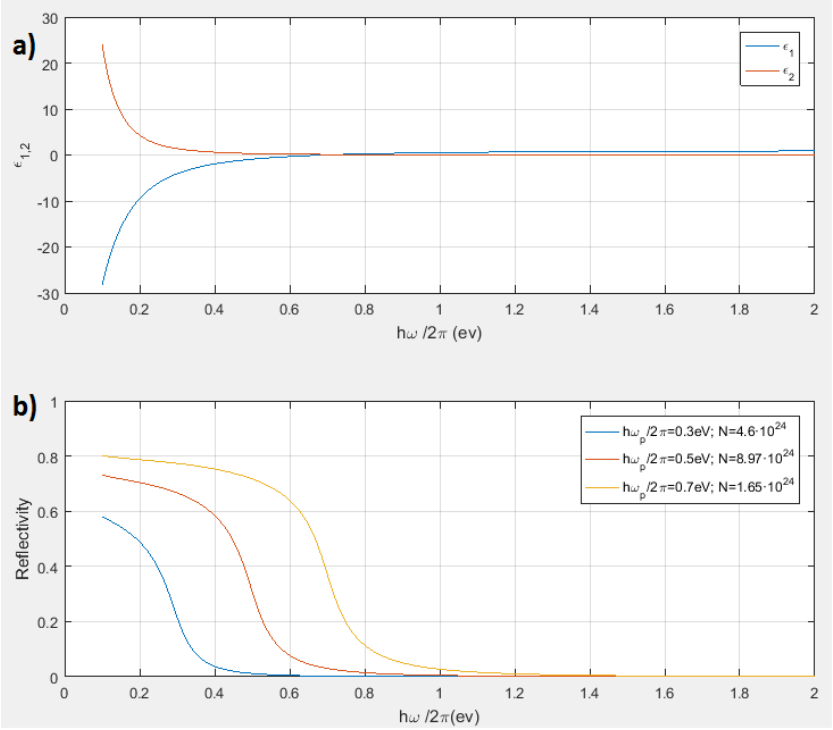

Figure 2. On a), it is shown the real (ϵ_1) and imaginary (ϵ_2) part from the dielectric constant where the plasma frequency ω_p is at 0.7eV. b) shows the reflectivity at different number densities N at $\omega_p = 0, 3; 0.5; 0.7$ eV.

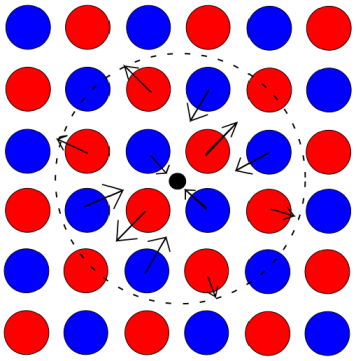

Figure 3. Schematic representation of a polaron. A free electron moving through an ionic lattice attracts the positive ions, and repels the negative ones. This produces a local distortion of the lattice within the polaron radius shown by the dashed circle.

For studying these ultrafast dynamics of nonequilibrium excitations, we are interested in measure in the MIR spectral range. In this region, it gives a strong absorption and reflection when it is considering the direct interaction between a light wave and the phonons in a solid.

However, it is challenging to characterize femtosecond pulses in this spectral region, therefore, my masters project will develop and method to do this.

2. Theory of FTIR

The Fourier Transform Infrared spectrometer (FTIR) is one of the most popular methods to characterize these excitations, which acquires broadband near-infrared (NIR) to far-infrared (FIR) spectra.

FTIR is a method of obtaining infrared spectra by first collecting an interferogram of a sample signal using an interferometer, and then, performing a Fourier Transform (FT) on the interferogram to obtain the spectrum. An FTIR spectrometer collects and digitizes the interferogram, performs the FT function, and displays the spectrum.

A Fourier Transform Infrared spectrometer uses the same basic configuration of mirrors and beamsplitter as a Michelson interferometer, where one of the mirrors can be moved rapidly back and forth, in this way we can make one measurement at different position of the mirror. This fast scanning mirror has several advantages. If the signal is noisy as a result of fluctuating background light, the frequency of the mirror motion can be chosen to be at a portion of the frequency spectrum for which the background fluctuations are less than at DC. In practice, mirror motions at a few tens of hertz will result in substantial noise reduction since noise amplitudes often drop off as $1/f$ or faster, where f is the frequency. Also, fast scanning times can mean data can be acquired rapidly. Due to this advantages, FTIR spectrometers have replaced dispersive IR spectrometers.

The name, FTIR, comes from the fact that the intensity measured by the diode $I_D(\Delta)$ of the recombined beam as a function of the path difference for light from the two arms, Δ, is the Fourier transform of the intensity of the light source, I(λ). [6] [7]

As we are dealing with pulsed light sources, we will work in the time domain in which case $\Delta = c\tau/2$ where c is the speed of light and τ is the time to travel a Δx distance in the movable mirror. The intensity measured by the diode is:

$$I_D(\tau) = \int EE^* dt \tag{1}$$

The amplitude of the combined beam can be written in complex form as:

$$E = E_0(t)\, e^{-i\omega t} + E_0(t+\tau)\, e^{-i\omega(t+\tau)} = \left(E_0(t) + E_0(t+\tau)\, e^{-i\omega\tau}\right) e^{-i\omega t} \tag{2}$$

Where $E_0(t)$ is the envelope of the function of the electric field, $\omega\tau$ is the phase difference between the two beams that results if they traverse paths of different lengths before recombining and ω is the central wavelength. The intensity measured by the diode of the combined beam (1):

$$\begin{aligned} I_D(\tau) &= \int EE^* dt = \int \left(E_0(t)\, e^{-i\omega t} + E_0(t-\tau)\, e^{-i\omega(t+\tau)}\right) \\ &\times \left(E_0(t)\, e^{i\omega t} + E_0(t-\tau)\, e^{i\omega(t+\tau)}\right) dt \\ &= \int E_0^2(t)\, dt + \int E_0^2(t-\tau)\, dt + 2\int E_0(t)\, E(t-\tau)\, cos(\omega\tau) \\ &= 2A + 2cos(\omega\tau) \int E(t)\, E(t-\tau)\, dt = 2A + 2cos(\omega\tau)\, \mathcal{F}(I(\omega)). \end{aligned}$$

Clarifying that: $\int E(t)\,E(t-\tau)\,dt = \mathcal{F}(I(\omega))$ where $\int E(t)\,E(t-\tau)\,dt = \mathcal{F}(E(\omega)\,E(\omega))$.

2.1. Choice of detector

In this project, we measure with a pulsed laser instead of a continuous wave laser. Therefore, in contrast to the continuous wave lasers, we detect a non continuous electric field supplied by each laser pulse.

In our home-built FTIR, we have to know which detector we are going to use. To measure in the infrared, the correct photodiode is made by indium gallium arsenide, InGaAs. It can detect light from 0.8 to 2.2 μm, also we can use the Mercury Cadmium Telluride (MCT) detector to measure from 3 to 10 μm. For reasons will be discussed later, we use a Silicon (Si) photodiode. As this photodiode can only measure between 0.3 and 1.1 μm, we add a BBO crystal to doubled the frequency.

On this case, the intensity measured by the diode is given by:

$$\begin{aligned} I_D^{(2\omega)}(\tau) &= \int E^{(2\omega)} E^{(2\omega)^*} dt \\ &= \int E_0^4(t)dt + \int 2E_0^2(t)E_0^2(t+\tau)cos(2\omega\tau)dt + \int 4E_0^3(t)E_0(t+\tau)cos(\omega t)dt \\ &+ \int E_0^4(t+\tau)dt + \int 4E(t)E_0^3(t+\tau)cos(\omega\tau)dt + \int 4E_0^2(t)E_0^2(t+\tau)dt. \end{aligned}$$

Where the oscillating terms are those with a cosines dependence. When the setup is badly aligned, these terms average to zero but it will always remain the $\int 4E_0^2(t)E_0^2(t+\tau)dt$ term that gives the envelope of the autocorrelation.

2.2. Laser source

The source we are going to characterise is given by a Ti:Sapphire laser whose central wavelength is 800 nm, 40 nm of bandwidth, the pulse energy is 1 mJ, its pulse duration of the laser is 35 fs, the repetition rate is 5 kHz. For infrared, a collinear optical parametric amplifier (OPA) where the pump is sent onto the nonlinear crystal and a down frequency conversion to lower frequencies, the signal and the idler, occurs spontaneously. We obtain a wavelength range from 1140 to 1600 nm (V polarization) from the signal and from 1600 to 2600 nm from the idler (H polarization).

2.3. Measurement

In the laboratory, we use a specific optical delay optic unit called *ScanDelay* as the fast scanning mirror of which we control the scan movement by its own software at 0.3 mm of amplitude of the triangular wave type that corresponds to 1 ps in time scale, and at 1 Hz of frequency.

To calculate the autocorrelation, each diode measurement will correspond to a specific mirror position, but the analogue to digital converter (ADC) digitise the whole

diode trace. After that, we extract each diode spike height just subtracting the minimum to the maximum voltage, obtaining the autocorrelation.

Firstly, we have to calculate the autocorrelation time, for that, we have to divide the total diode readings in a scan per the diode readings per second. In a LabVIEW programme, we set these number as fast as the ADC can read, in this case we have 10^6 diode readings in a scan and $2 \cdot 10^6$ diode readings per second, so, the time for a scan is $t = 0.5$ *seconds*. For the maximum sampling rate $\frac{0.5}{2 \cdot 10^6} = 0.25\mu$s, the InGaAs photodiode response is faster than this time, so it cannot be analysed by the ADC, for that reason, we choose the Si photodiode whose response is slower to 0.25 μs and we can detect its diode trace. To know how many pulses are in t time, we only have to calculate the time we calculated per the laser frequency: $\frac{time}{laser\ \ frequency} = 0.5s \times 5000s^{-1} = 2500$ pulses. Finally, to know how many points per pulse we have, we just divide the total diode readings in scan per the number of pulses: $\frac{total\ \ diode\ \ readings\ \ in\ \ scan}{number\ \ of\ \ pulses} = \frac{2 \cdot 10^6}{2500} = 800$ points per pulse.

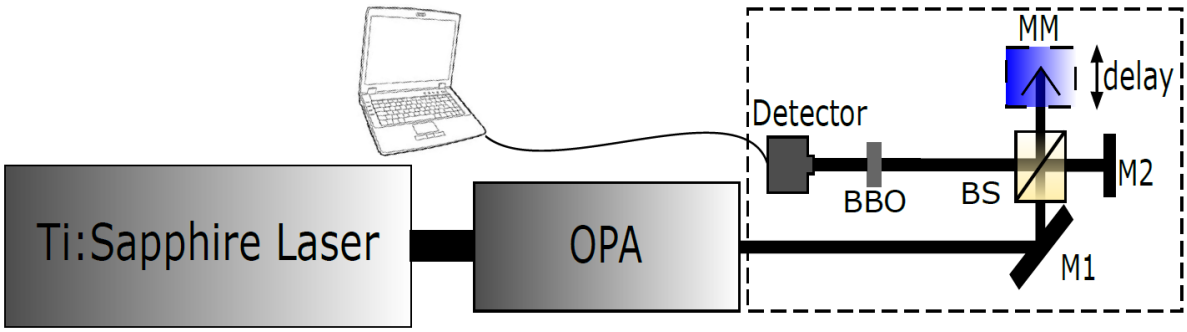

Figure 4. Schematic setup to characterise a pulse formed by the Ti:Sapphire Laser, OPA, two fixed mirror (M1) and (M2), a beamsplitter (BS), a movable mirror (MM) that creates the delay, a BBO crystal, a photodiode (detector) and a computer to analyse all the data. The dashed rectangle shows the interferometer.

An schematic figure of the autocorrelation measurement at each τ_i time is shown in figure 5.

3. Results

The measurements in the IR region are difficult so in this section we present the results obtained for the diode trace, the pulse duration and the central wavelength of the pulse in the visible region.

The whole diode trace and autocorrelation measured in figure 6 and figure 7 show the digitalization of the schematic figure 5 at 1300 nm of central wavelength from the OPA. In both figures, we only see the envelope of the autocorrelation, without the oscillation terms; and the insert of figure 6 shows zoom of the trace showing the individual diode traces. The dashed rectangle shows the individual diode trace from where we calculate the height of the peak subtracting the minimum to the maximum voltage.

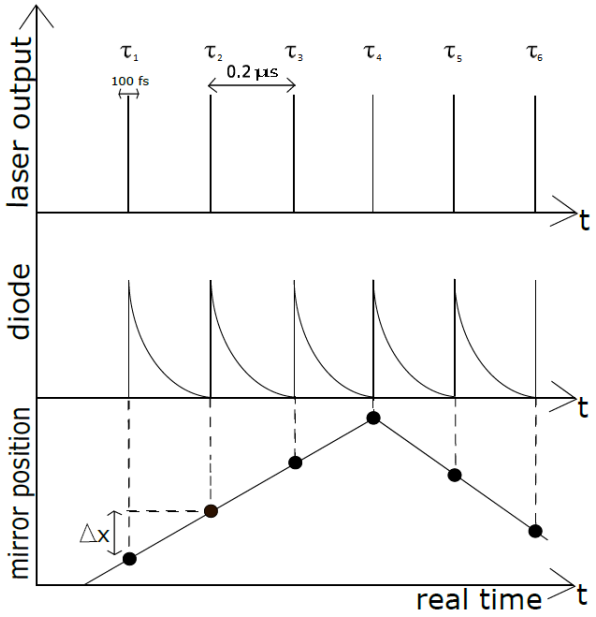

Figure 5. As the laser output is too fast, $\sim$ 100 fs, we only measure the diode response at different mirror positions. τ_i is the time that the mirror takes to go to a Δx position and t is the time in the laboratory frame.

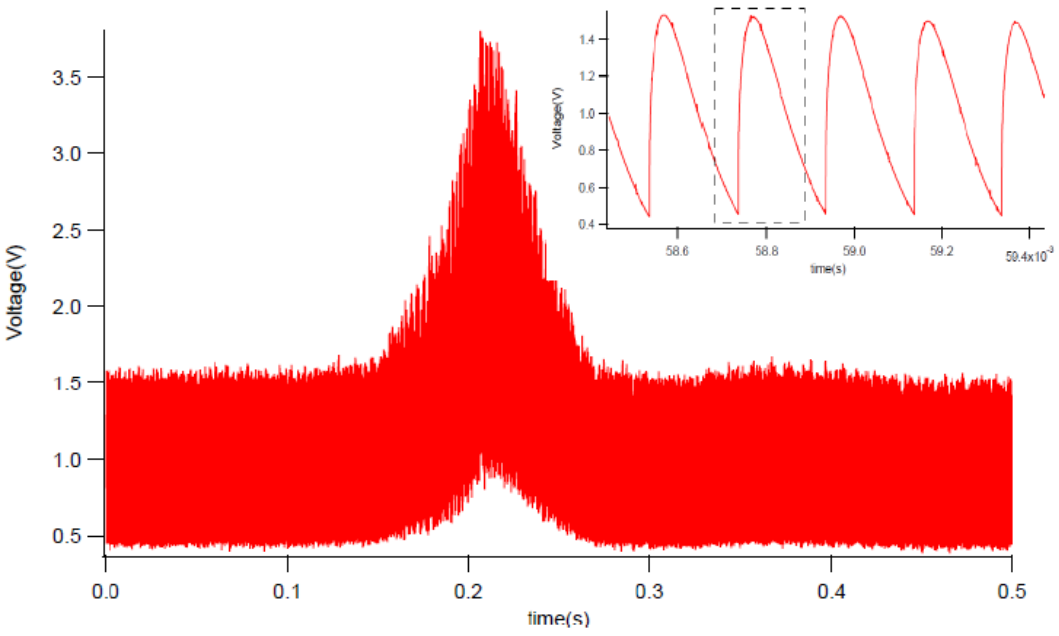

Figure 6. 0.5 second reading of the diode signal at 1300 nm of central wavelength. The insert shows a zoom of the trace showing the individual diode traces.

To measure the pulse duration, we plot the amplitude values of the diode spike to obtain the autocorrelation, which is the one we are interested in measure. As well as before, we measure at 1 ps of amplitude of the triangular wave type and at 1 Hz of frequency. To calculate the x axis, we suppose that the triangular wave is perfectly

linear and knowing that at the half of the frequency (1) Hz we have 1 ps of amplitude, we can calculate the slope of this triangle function. With this value and knowing there is a laser pulse every $\frac{1}{5000Hz} = 200\mu$s we can calculate that there is a point on the plot every 0.04 fs.

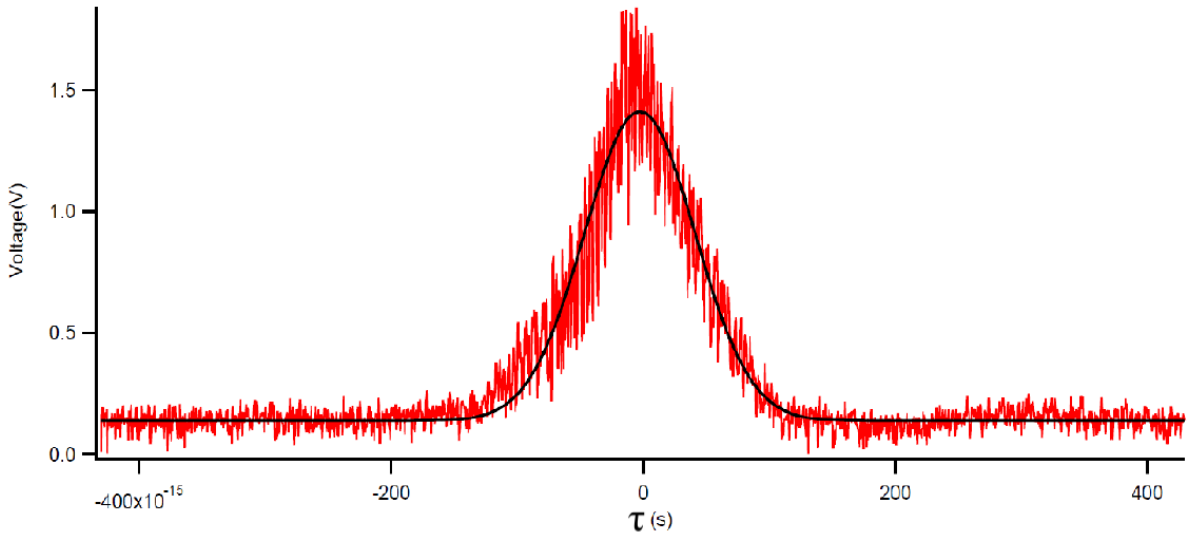

Figure 7. Peak measurement by calculating the amplitude of each diode spike at 1300 nm of central wavelength.

Then, to calculate the pulse duration, we fit the peak into a gaussian peak (Figure 7) by a data analysis programme called *Igor* that tells to us the width of the autocorrelation.

To measure the pulse duration, we need to know the full width at half maximum (FWHM). The autocorrelation of two gaussian functions gives another gaussian function:

$$y = e^{\left(\frac{FWHM}{2 \cdot width}\right)^2}$$

Where "width" is the width of the autocorrelation. At half maximum $y = \frac{1}{2}$:

$$\frac{1}{2} = e^{\left(\frac{FWHM}{2 \cdot width}\right)^2} \Rightarrow ln2 = \frac{FWHM^2}{4width^2} \Rightarrow FWHM = 2width \cdot \sqrt{ln2}.$$

In this case, for the shown peak in Figure 7 the width of the autocorrelation is $width = 1.2386 \cdot 10^{-13} seconds$.
Substituting this value into the FWHM equation we obtain:

$$FWHM = 2\sqrt{ln2} \cdot 1.2386 \cdot 10^{-13} = 206 fs.$$

But we should to note that the FWHM of the autocorrelation is not the FWHM of the pulse so we need to divide by $\sqrt{2}$.

Finally, the pulse duration of the pulse is:

$$FWHM_{peak} = \frac{206}{\sqrt{2}} = 146 fs.$$

This result is close to what we expected. The broadening of the pulse is due to the OPA process and as a result of the beam goes through certain materials.

Now, to see the fringes in the autocorrelation, we make the length of the arms from the interferometer longer and we measure at longer wavelengths to have less stability to improve the alignment of the setup. At 1500 nm instead of 1300 nm of central wavelength from OPA we can see the oscillation terms from $I_D^{(2\omega)}(\tau)$ in the autocorrelation.

To measure the central wavelength we calculate the Fourier transform of the pulse shown in the insert of figure 8, in this way we obtain the information of the wavelengths. In the laboratory, we control the scan movement at 1 ps of amplitude of the triangular wave type and at 1 Hz of frequency.

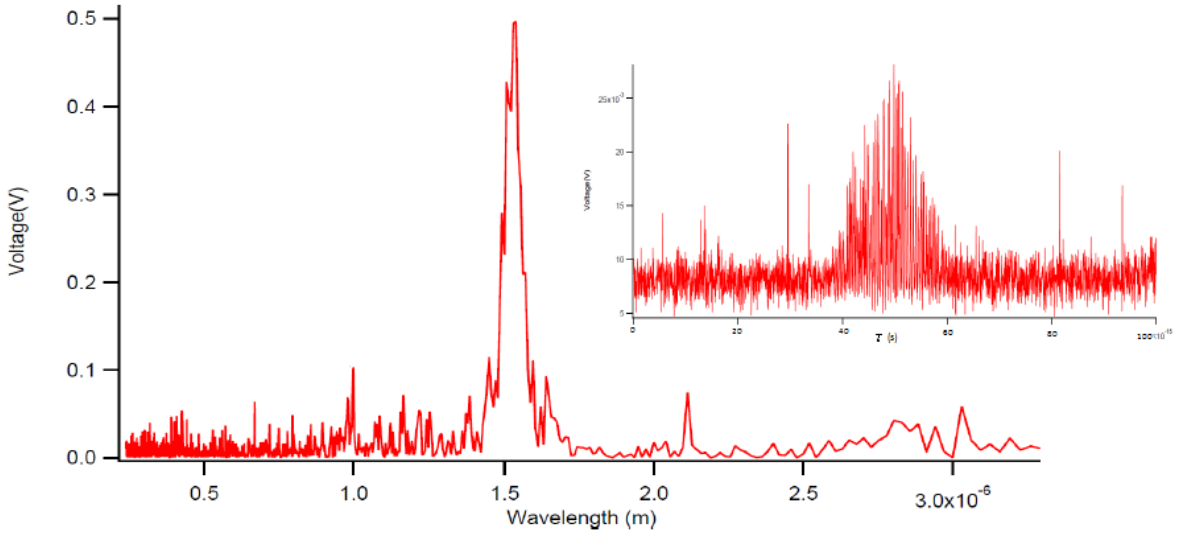

Figure 8. Fourier transform of the peak measurement at 1500 nm of central wavelength from the OPA. In this way, we obtain information of this central wavelength. The insert shows the corresponding autocorrelation measurement.

We can see in figure 8 the central wavelength is at 1538 nm that is very close to the 1500 nm expected.

4. Conclusions

To understand the physics of solids, it is important to observe how light interacts with them. In the mid-infrared region, it gives a strong absorption and reflection when it is considering the direct interaction between a light wave and the phonons in a solid. In this spectral region, it is challenging to characterize femtosecond pulses. In this masters project, it has been built an FTIR. We demonstrated the functionality of this spectrometer by measuring the autocorrelation, the pulse duration and the central wavelength of the pulse in the visible region instead of the infrared one. If we want to measure in the infrared region, we just have to change the Si to the InGaAs photodiode,

taking into account that the decay constant of the photodiode has to be slower than 0.25 μs.

5. References and notes.

[1] B. E. Saleh and M. C. Teich, *Fundamentals of photonics*, vol. 22. Wiley New York, 1991.
[2] "Class notes, Condensed Matter Physics, Present the Drude model, Universidad de Cordoba, 2014."
[3] M. Dressel and G. Guner, *Electrodynamics of solids*. Cambridge University Press, 2005.
[4] M. Fox, *Optical properties of solids*, vol. 3. Oxford university press, 2010.
[5] R. W. Wyckoff, *Crystal structures*, vol. 2. Interscience New York, 1960.
[6] E. Hecht, *Optics*, vol. 997. 1998.
[7] J. F. James, *A student's guide to Fourier transforms: with applications in physics and engineering*. Cambridge university press, 2011.